

**EJECTA DEPOSITS BEYOND THE LAYERED EJECTA RAMPART ON MARS: IMPLICATIONS FOR EJECTA EMPLACEMENT AND CLASSIFICATION.** L. L. Tornabene<sup>1</sup>, J. L. Piatek<sup>2</sup>, N. G. Barlow<sup>3</sup>, A. Bina, R. Capitan, K. T. Hansen<sup>1</sup>, A. S. McEwen<sup>5</sup>, G. R. Osinski<sup>1,4</sup>, and S. J. Robbins<sup>6</sup>, <sup>1</sup>Centre for Planetary Science & Exploration (CPSX) and Dept. of Earth Sciences, Western University (1151 Richmond Street, London, ON N6A 5B; [ltornabe@uwo.ca](mailto:ltornabe@uwo.ca)), <sup>2</sup>Dept. of Geological Sciences, Central Connecticut State Univ., New Britain, CT, <sup>3</sup>Dept. Physics and Astronomy, Northern Arizona Univ., Flagstaff, AZ, <sup>4</sup>Dept. of Physics and Astronomy, Western University, London, ON, <sup>5</sup>LPL, University of Arizona, Tucson, AZ, and <sup>6</sup>Southwest Research Institute, Boulder, CO.

**Introduction:** “Radial” crater ejecta represents the most common ejecta morphologic type on the Moon and Mercury [1], while on Mars, the “layered” ejecta class is the most dominant morphology (>90% for craters  $\geq$  5 km in diameter) [2,3]. Volatile content within (or on) the target [e.g., 4] and/or effects from the interaction of the ejection process with the atmosphere [e.g., 5] have been proposed to explain the resulting layered ejecta morphology. Layered ejecta is also distinct from the radial class of ejecta with respect to its morphometric profile [e.g., 6], which includes a characteristic distal ridge or scarp, commonly referred to as a “rampart” [4,7-8]. Importantly, this ejecta rampart has often been assumed to be the terminus of the continuous ejecta and the start of the discontinuous ejecta.

Here we report on observations and mapping results based on HiRISE [9] and CTX [10] images the best-preserved simple-to-complex transitional craters on Mars [see 11-13]. Our results provide evidence of a relatively thin, but distinctive and continuous flow-ejecta facies beyond the layered ejecta rampart that is sourced from abundant crater-related pitted and smooth deposits commonly observed atop the ballistic ejecta facies, and interpreted to be volatile-rich impact melt-bearing deposits [see 14-16]. Hence, it appears that the pitted and smooth deposits and the flow facies described here together constitute a second layer of ejecta consistent with [16]. The observations and interpretations presented here may change where we demarcate the continuous and discontinuous ejecta, how we classify ejecta, and begin to answer questions regarding the relationships, mechanism(s) involved, and the timing of ejecta emplacement.

**Background and General Methods:** Emphasized in this abstract are the morphological mapping results for one of the best-preserved simple-to-complex transitional Single Layer Ejecta (SLE) craters on Mars: Resen. Resen is approximately 7.6 km in diameter and located in Hesperia Planum ( $108.88^{\circ}$ E,  $27.94^{\circ}$ S). The SLE ejecta of Resen is rather short, with a runout distance of only  $\sim$ 3 km on average ( $\sim$  0.75 crater radii). Resen was selected based on the general characteristics outlined in [11-13], including a target with less topographic variation (i.e., Hesperian-ridged plain materials) and as an example of a transitional crater that has experienced the least amount of post-impact modification for its size class. To better understand the transition

from continuous to discontinuous ejecta, we specifically targeted and acquired long HiRISE images ( $\sim$ 100-120k lines) that start at the layered ejecta rampart edge and align with a radial traverse from the crater (Fig. 1). These observations were not only key for providing high-resolution meter- to decameter-scale detail, but also provided the continuous context needed to best observe and characterize these additional ejecta facies beyond the layered ejecta rampart of Resen.

It is important to note that we observe similar patterns in HiRISE and CTX observations of other examples of the best-preserved craters on Mars (e.g., Noord, Gratteri, Zunil, Tooting, etc.); therefore, we emphasize that results of this work do not appear to be unique to Resen.

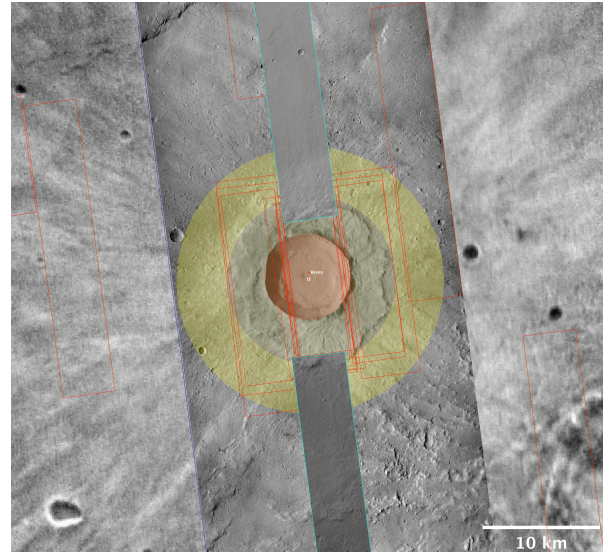


**Fig. 1.** HiRISE coverage (red) of Resen crater highlighting two (one north – ESP\_050674\_1520 and one south – ESP\_049751\_1515) long ( $>100$ k lines) images that are radial to Resen. The yellow circle shows the approximate bounds of the bulk of the additional continuous ejecta ( $\sim$ 6 km from the rim with portions found up to  $\sim$ 12 km).

All Mars datasets were imported as an ArcGIS-project into ArcMap, with a hierarchy of HiRISE, CTX, THEMIS, HRSC DTMs (if available) and MOLA MEGDR as a basemap. Mapping focused on HiRISE with comparisons to both CTX and THEMIS-derived thermal inertia [17] images. Based on meter- to decameter-scale texture, tone, relief, and structure, various features were defined as morphologic units/facies, traced as vector polygon layers, and symbolized by specific

colours. The classes were later adjusted based on our observations and interpretations of the initially defined units to illustrate similarities and emphasize differences between groups of units (e.g., related units being different shades of the same colour).

**Observations:** HiRISE and CTX observations show that there are multiple continuous flows that emanate from the ponded & pitted and smooth & flowing deposits [14-15] that lie atop the layered ejecta facies. These numerous flows coalesce into a continuous flow deposit for an additional ~2 – 3 crater radii from the layered ejecta rampart, or ~3 – 4 radii from the rim). The facies of ejecta that lies beyond the rampart is continuous and generally characterized by smooth and gentle to undulating (possibly inter-fingering?) flows that embay quasi-radial hummocky terrains. The flow facies observed here is somewhat similar to Low-Aspect Ratio Layered Ejecta (LARLE) [18-19], with the exception of having much shorter run-outs (<6 crater radii) and it possesses superior preservation. The flows most proximal to the rampart are marked by numerous elongated clusters of pits that are quasi-radial to the primary. The proximity to the primary and their sinuous, even curved nature with respect to obstacles, are inconsistent with secondary crater chains (buried or otherwise). The flow facies terminates in multiple lobes that where they generally lack the pit clusters commonly observed closer to the rampart, and instead are marked by numerous striae that are radial to the primary. There are also numerous discrete rougher and higher-standing hummocky terrains observed within the flow facies as isolated or quasi-linear chains that also appear to be quasi-radial to the primary. They are notably coated and embayed by the smooth and pitted flow materials, and thus are interpreted to predate the emplacement of the flow facies. They are almost identical in appearance to hummocky terrains that are larger and more abundant within the layered ejecta facies. Mapping results indicate that these hummocky terrains occur circumferentially, and are confined within a certain radial distance, to the primary crater. As such, we interpret them to be portions of the ballistic ejecta blanket that generally underlies the flow-ejecta facies. Indeed, we note that pre-impact target-surface features are rare and are often absent within the margins of the flow facies.

The most characteristic feature of this facies of ejecta is the lack of pre-impact target surfaces, herringbone patterns and secondary crater chains crater-ward of its margins. It is not until the terminal striated lobes of the flow facies is reached that we begin to observe more abundant partially buried and scoured herringbone patterns, secondary crater chains and target-surface features. With increasing distance from this boundary, the secondaries become less and less buried and scoured in

appearance until they are at their sharpest and deepest appearance. Based on our mapping of Resen, this occurs ~13-17 km (~3 – 4.5 radii) beyond the crater rim.

We suggest that the terminal lobes and the emergence of these features marks the true contact between continuous ejecta and discontinuous ejecta.

**Timing of ejecta emplacement and “self”-modification:** Based on our mapping results and stratigraphic relationships observed in HiRISE images, we suggest a sequence in the emplacement of ejecta facies (from the earliest to latest) of: (1) vapor plume blast winds associated scour and sediment transport [see 20] (2) herringbone patterns and secondaries, (3?) ejecta curtain winds associated with scouring/deposition, (4) ballistic/radial hummocky ejecta → layered ejecta/rampart formation, (5) ponded & pitted/smooth & flowing deposits (incorporation and modification of ballistic ejecta), (6) flow facies beyond the layered rampart (continued ballistic ejecta modification), (7) pits associated with previous, additional flows post-emplacement due to slopes/topography, and (8) minor aeolian modification based on the prevailing wind-direction in the region.

**Future work:** Additional mapping, morphometry based on HiRISE stereo, measurements (e.g., EM of flow facies) and mapping/imaging of additional craters at larger diameters are planned as part of our future research on this topic.

**References:** [1] Barlow N.G. et al. (2000), *JGR*, 105, 26733-26738. [2] Barlow N.G. (1988), *Icarus* 75, 285–305. [3] Barlow N.G. et al. (2007), *7<sup>th</sup> Mars*, [4] Carr et al. (1977), *JGR* 82, 4055-4065. [5] Schultz P.H. and Gault D.E. (1979), *JGR*, 84, 7669-7687. [6] Komatsu et al. (2007), *Icarus*, 112. [7] McCauley J.F. (1973), *JGR* 78, 4123-4137. [8] Mouginis-Mark P.J. (1977), *JGR*, 84, 8011-8022. [9] McEwen A.S. et al. (2007), 112. [10] Malin M.C. et al. (2007), *JGR*, 112. [11] Tornabene L. L. et al. (2015). *LPSC 46*, Abstract #2531. [12] Tornabene L.L. et al (2016) *LPSC 47*, Abstract #2879. [13] Piatek J. L. et al (2015) *LPSC 46*, Abstract #2654. [14] Tornabene L.L. et al. (2012), *Icarus* 220, 348–368. [15] Boyce J.M. et al. (2012) *Icarus* 221, 262-275. [16] Osinski G.R. et al. (2011), *EPSL*, 310, 167-181. [17] Christensen et al. [18] Barlow N.G. et al. (2014), *JGR*, 239, 186–200. [19] Boyce J.M. et al. (2015) *Icarus*, 245, 263-272. [20] Schultz P.H. and Quintana S.N. (2017), *Icarus*, 292, 86-101.

**Acknowledgements:** The authors wish to thank NASA’s Mars Data Analysis Program (NNX15AM41G) for supporting this work, and acknowledge Tornabene’s personal Canadian-based support from the NSERC Discovery Grant programme (RGPIN/04215-2014) and the Canadian Space Agency (CSA) (14EXPUWO-002).